Cardiovasc Intervent Radiol (2019) 42:448–454
https://doi.org/10.1007/s00270-018-2123-9

Lymphangiography and Post-lymphangiographic Multidetector CT for Preclinical Lymphatic Interventions in a Rabbit Model

Tomohiro Matsumoto[1,2] · Kosuke Tomita[1] · Shunto Maegawa[1,2] · Takako Nakamura[3] · Tetsuya Suzuki[2] · Terumitsu Hasebe[1,2]

Received: 10 July 2018 / Accepted: 12 November 2018 / Published online: 20 November 2018

Abstract

Purpose To describe the feasibility of lymphangiography and the visibility of the lymphatic system using post-lymphangiographic multidetector CT (MDCT) for preclinical lymphatic interventions in a rabbit model.

Materials and Methods Lymphangiography via the popliteal lymph node or vessel after surgical exposure was performed, using six healthy female Japanese White rabbits. Lipiodol was manually injected for lymphangiography. Post-lymphangiographic MDCT examinations were performed in all rabbits. The dataset images were subjected to image processing analysis utilizing the three-dimensional maximum intensity projection technique. Three reviewers evaluated the degree of depiction of the lymphatic system using a four-point visual score (1, poor; 2, fair; 3, good; 4, excellent). The distance between the body surface and cisterna chyli was measured on post-lymphangiographic MDCT axial image.

Results Lymphangiography was successfully performed in all rabbits. The popliteal lymph node was detectable in 90%. The visualization of lymphatic system via the popliteal node was achieved in 89%. Mean visual scores of > 3.0 were realized by the right femoral lymphatic vessel, left femoral lymphatic vessel, left iliac lymphatic vessel, left lumbar lymphatic trunks and cisterna chyli, whereas mean visual scores of < 3.0 were yielded by the right iliac lymphatic vessel, right lumbar lymphatic trunks and thoracic duct. The distance between the body surface and cisterna chyli on post-lymphangiographic MDCT axial images was 4.33 ± 0.14 cm.

Conclusion Lymphangiography is feasible, and the visibility of the lymphatic system on post-lymphangiographic MDCT in a rabbit model provides enough information for interventional radiologists to perform preclinical lymphatic interventions.

Electronic supplementary material The online version of this article (https://doi.org/10.1007/s00270-018-2123-9) contains supplementary material, which is available to authorized users.

Tomohiro Matsumoto and Terumitsu Hasebe have contributed equally to this work.

✉ Terumitsu Hasebe
hasebe@tokai-u.jp

Tomohiro Matsumoto
t-matsu@tokai-u.jp

Kosuke Tomita
ktomita@tsc.u-tokai.ac.jp

Shunto Maegawa
s.ifor800@z3.keio.jp

Takako Nakamura
takako-nakamura@aist.go.jp

Tetsuya Suzuki
tsuzuki@mech.keio.ac.jp

[1] Department of Radiology, Tokai University Hachioji Hospital, Tokai University School of Medicine, 1838 Ishikawa-machi, Hachioji, Tokyo 192-0032, Japan

[2] Center for Science of Environment, Resources and Energy, Graduate School of Science and Technology, Keio University, 3-14-1 Hiyoshi, Kohoku-ku, Yokohama, Kanagawa 223-8522, Japan

[3] Advanced Coating Technology Research Center, National Institute of Advanced Industrial Science and Technology, Tsukuba, Ibaraki 305-8565, Japan

Keywords Lymphangiography · Post-lymphangiographic multidetector CT · Lymphatic interventions · Lipiodol

Introduction

The number of reports on lymphatic interventions including pedal or intranodal lymphangiography for detecting or treating lymphatic leaks [1–7] and thoracic duct embolization for postoperative chylothorax [8–11] has been increasing. However, lymphatic leakage remains a challenging clinical problem with high mortality in post-esophageal surgery [12]. Furthermore, while lymphangiography and thoracic duct embolization offer an attractive and viable alternative to surgery, the technique is demanding, and the requisite expertise is not always widely available [12].

Despite this problem, a universal animal model for lymphatic interventions has not yet been developed. There have been a limited number of reports on the swine model of intranodal lymphangiography using Lipiodol (Andre Guerbet, Aulnay-Sous-Bois, France) [13] and thoracic duct embolization [14]. While it is true that the swine model mimics human lymphatics, swine have higher maintenance costs and are harder to handle than rabbits. Specialized infrastructure and trained personnel are therefore a prerequisite for the experimental study in swine. On the other hand, rabbits are inexpensive, easy to manage in a laboratory setting and have an organ system like that of humans. Rabbits had been used in lymphangiography utilizing only X-ray imaging without multidetector CT (MDCT) imaging in a previous study [15]. With the advent of MDCT, image resolution has increased owing to thinner collimation. The high-quality image data forthcoming can be processed further into multiplanar reformatted (MPR) or maximum intensity projection (MIP) images and three-dimensional volumetric (3D) images. Therefore, the objective of our present study is to describe the feasibility of lymphangiography and the visibility of the lymphatic system on post-lymphangiographic MDCT for preclinical lymphatic interventions in rabbits.

Materials and Methods

Animal Models

The study was approved by the institutional Animal Care and Use Committee of Tokai University. Six healthy female Japanese White rabbits weighing 3.0–3.5 kg (Tokyo Laboratory Animals Science Co., Ltd., Tokyo, Japan) were used. During lymphangiography, all rabbits were anesthetized with 3.0% isoflurane.

Lymphangiography Protocol (Fig. 1)

Initially, we performed the intranodal lymphangiography via the right popliteal lymph node in all rabbits. All rabbits were supine positioned, and intracutaneously injected with 0.1 mL of 1% patent blue violet dyes (Fisher Scientific Corp., Shirley, NY) into the right bottom of the foot to facilitate the identification of the popliteal lymph node and lymphatic vessel. Linear cut-down was performed 5 min later on the right popliteal fossa between the biceps femoris and the semimembranosus, and the right popliteal node was isolated. After the puncture of the right popliteal node using a 30-gauge needle for lymphangiography (Hakko Medical, Tokyo, Japan) (Fig. 2), the insertion site was immediately fixed by a medical tissue glue, Aron-alpha-A (Daiichi Sankyo, Tokyo, Japan). After the fixation procedure, Lipiodol was warmed to 40 degrees Celsius (°C), using it as a contrast agent for lymphangiography, with manual injection at a rate of 0.1 mL over 2–3 min with a 2.5-mL syringe (Terumo, Tokyo, Japan). The total volume of Lipiodol was 1 mL. After injecting 1 mL of Lipiodol, we confirmed the transport of Lipiodol through the lymphatic system under fluoroscopy. When Lipiodol had reached the left venous angle, which we defined as the inflow part of a Lipiodol droplet into the venous system under fluoroscopy, the rabbits were euthanized by excess pentobarbital administration to stop lymphatic flow. When Lipiodol had reached the cisterna chyli or thoracic duct, we waited for the natural flow of lymph to carry Lipiodol up through the thoracic duct before the rabbits were euthanized by excess pentobarbital administration. Intranodal lymphangiography via the left popliteal lymph node was carried out in the same way as described above when Lipiodol had reached only the femoral lymphatic vessel, iliac lymphatic vessel, or lumbar lymphatic trunks under fluoroscopy, or when the lymphatic system had not been visualized under fluoroscopy or the right popliteal lymph node had not been detectable. In one of the remaining rabbits, it was not possible to detect the left popliteal lymph node, and therefore the lymphangiography procedure via a left popliteal lymphatic vessel was performed. After the left popliteal lymphatic vessel was isolated, the surrounding tissues were stripped, thereby giving good access to the lymphatic vessel, which was then cannulated. Next, lymphangiography was carried out in the same way as described above. The rabbits were euthanized by excess pentobarbital administration after injecting 1 mL of Lipiodol through the left popliteal lymph node or left popliteal lymphatic vessel in the same process of fluoroscopy evaluation.

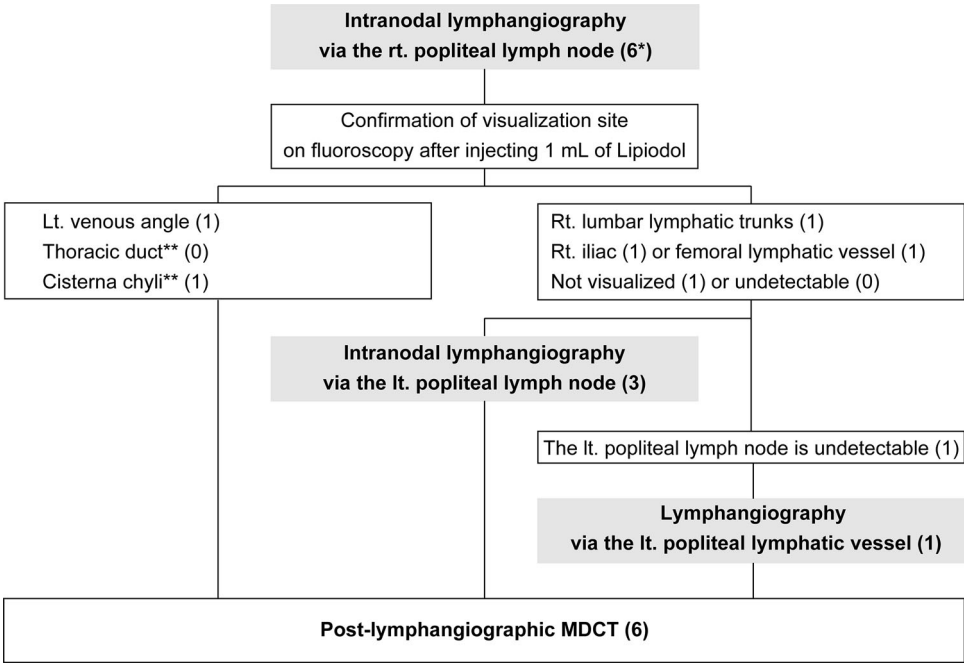

Fig. 1 Flowchart showing the lymphangiography protocol used in this study. *The number of rabbits is shown in parentheses. **After Lipiodol has reached the cisterna chyli or thoracic duct just after injection of 1 mL of Lipiodol via the rt. popliteal lymph node, the right venous angle is visualized by the transport of Lipiodol through the lymphatic system. *Rt.* right, *lt.* left, *MDCT* multidetector CT

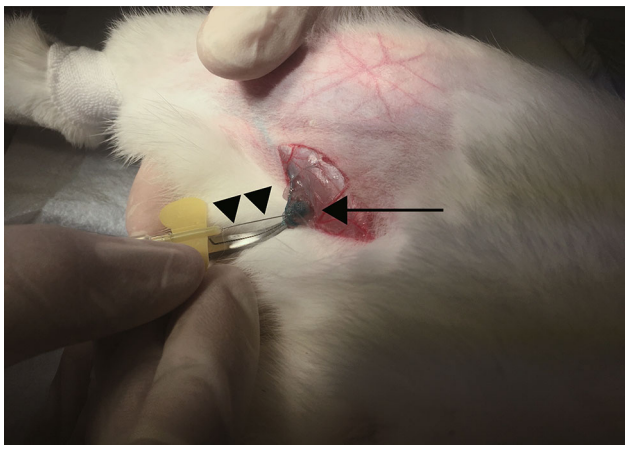

Fig. 2 Picture showing a 30-gauge needle for lymphangiography (arrowheads) inserted into right popliteal lymph node (arrow)

Post-lymphangiographic MDCT Examinations

Post-lymphangiographic 128-row MDCT (SOMATOM Definition Edge; Siemens Medical Solutions, Inc., Forchheim, Germany) examinations were performed in all rabbits. Images were acquired with the following parameters: 0.6 mm thickness, 512 × 512 matrices, 120 kV, 77 mAs, 0.5 s/rot.

3D MIP Image Postprocessing

The Digital Imaging and Communications in Medicine (DICOM) files were imported into OsiriX v.2.8.1 64-bit image processing software (Pixmeo, Geneva, Switzerland) for Macintosh. The dataset images were subjected to image processing analysis by use of the 3D MIP technique.

Image Analysis

All 3D MIP images were independently analyzed by three radiologists. Reviewer 1 (T.M.) had 15 years of experience; reviewer 2 (T.H.), 21 years of experience; and reviewer 3 (K.T.), 6 years of experience. Reviewers evaluated the degree of depiction of the femoral lymphatic vessel, iliac lymphatic vessel, lumbar lymphatic trunks, cisterna chyli, and thoracic duct using a four-point visual score. For these lymphatics, a score of 4 indicated excellent delineation with no structural discontinuity along the full length; 3, good delineation with minimal discontinuity; 2, fair delineation with some acceptable discontinuity; and 1, poor delineation with markedly unacceptable discontinuity. Moreover, interobserver reliability for the overall lymphatic visualization was calculated using the Cohen kappa coefficient.

We measured the distance between the body surface and cisterna chyli on post-lymphangiographic MDCT axial images.

Results

Lymphangiography was successfully performed in all rabbits. In one rabbit (Fig. 1), Lipiodol reached the left venous angle under fluoroscopy just after injecting 1 mL of Lipiodol via the right popliteal lymph node (Fig. 3A). In

one rabbit (Fig. 1), Lipiodol reached the cisterna chyli under fluoroscopy just after injecting 1 mL of Lipiodol (Fig. 3B). The left venous angle was visualized 1 min after injecting 1 mL of Lipiodol additionally via the right popliteal lymph node (Fig. 3B). In three out of the remaining four rabbits (Fig. 1), intranodal lymphangiography via the left popliteal lymph node was performed because Lipiodol, which was injected via the right popliteal lymph node, had reached only the right femoral lymphatic vessel in one rabbit and the right iliac lymphatic vessel in one rabbit (Fig. 3C); and no visualization of lymphatics was found in one rabbit because of extravasation of the total dose of Lipiodol around the right popliteal lymph node (Fig. 4). In the only remaining rabbit (Fig. 1), lymphangiography via the left popliteal lymphatic vessel was carried out because it was not possible to detect the left popliteal lymph node. The popliteal lymph node was detectable in 9/10 (90%) (Table 1). The popliteal lymph node maximum diameter was 7.2 ± 1.9 (5–11) mm (Table 1). Leakage of total (Fig. 4) or partial dose of Lipiodol around the popliteal lymph node was found in 7/9 (78%). The visualization of the lymphatic system via the popliteal node was 8/9 (89%) on the 3D MIP image (Figs. 4 and 5).

Mean visual score of the three reviewers decreased in order from the femoral lymphatic vessel, iliac lymphatic vessel to lumbar lymphatic trunks on the 3D MIP image (Table 2). Mean visual scores of > 3.0 were realized by the right femoral lymphatic vessel, left femoral lymphatic vessel, left iliac lymphatic vessel, left lumbar lymphatic trunks and cisterna chyli, whereas mean visual scores of < 3.0 were found for the right iliac lymphatic vessel, right lumbar lymphatic trunks and thoracic duct on the 3D MIP image (Table 2). The Cohen kappa coefficient between reviewer 1 and 2, 2 and 3, and 1 and 3 was 0.916 (95% confidence interval [CI] 0.834–0.998), 0.757 (95% CI 0.633–0.882), and 0.838(95% CI 0.736–0.941), respectively.

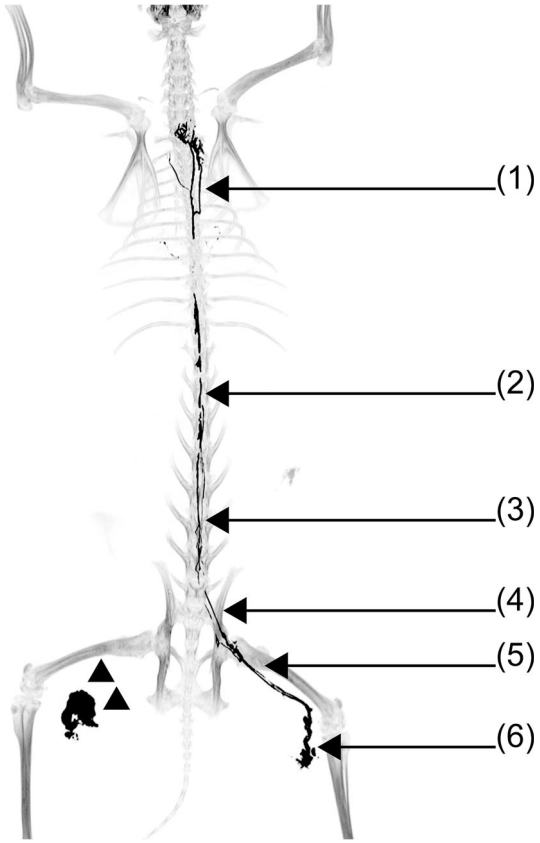

Fig. 4 Three-dimensional maximum intensity projection (3D MIP) image on post-lymphangiographic multidetector CT in anteroposterior view showing the lymphatic system in a rabbit: (1) thoracic duct, (2) cisterna chyli, (3) left lumbar lymphatic trunks, (4) left iliac lymphatic vessel, (5) left femoral lymphatic vessel, (6) left popliteal lymph node. Note that no visualization of lymphatics was found in the rabbit because of the extravasation of total dose of Lipiodol around the right popliteal lymph node (arrowheads)

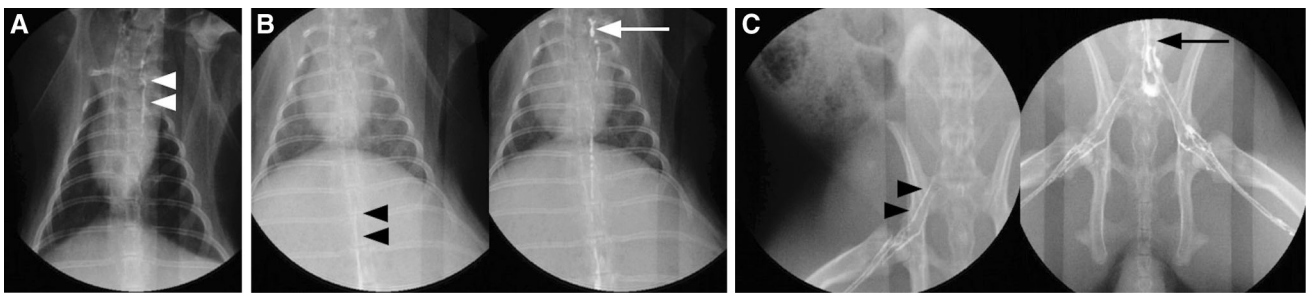

Fig. 3 Lymphangiography under fluoroscopy in rabbits. **A** Fluoroscopic image in anteroposterior view showing Lipiodol reaching the left venous angle (white arrowheads). **B** Fluoroscopic images in anteroposterior view, showing: (left) Lipiodol reaching only cisterna chyli just after injecting 1 mL of Lipiodol via the right popliteal lymph node (black arrowheads); and (right) the right venous angle as visualized 1 min after injecting 1 mL of Lipiodol via the right popliteal lymph node (white arrow). **C** Fluoroscopic images in anteroposterior view; showing: (left) Lipiodol injected via the right popliteal lymph node reaching only the right iliac lymphatic vessel (black arrowheads); and (right) left lumbar lymphatic trunks (black arrow) and iliac lymphatic vessel found after injecting Lipiodol via the left popliteal lymph node

Table 1 Identification and diameter of respective popliteal nodes

Rabbit No.	Right popliteal lymph node	Diameter of right popliteal lymph node (mm)	Left popliteal lymph node	Diameter of left popliteal lymph node (mm)
1	Detectable	5	Detectable	7
2	Detectable	5	Detectable	7
3	Detectable	9	Detectable	8
4	Detectable	6	N/A	N/A
5	Detectable	11	Undetectable[a]	N/A
6	Detectable	7	N/A	N/A

[a]Lymphangiography via the left popliteal lymphatic vessel was carried out because it was not possible to detect the left popliteal lymph node

No. number, *N/A* not applicable

The distance between the body surface and cisterna chyli on post-lymphangiographic MDCT axial image was 4.33 ± 0.14 cm.

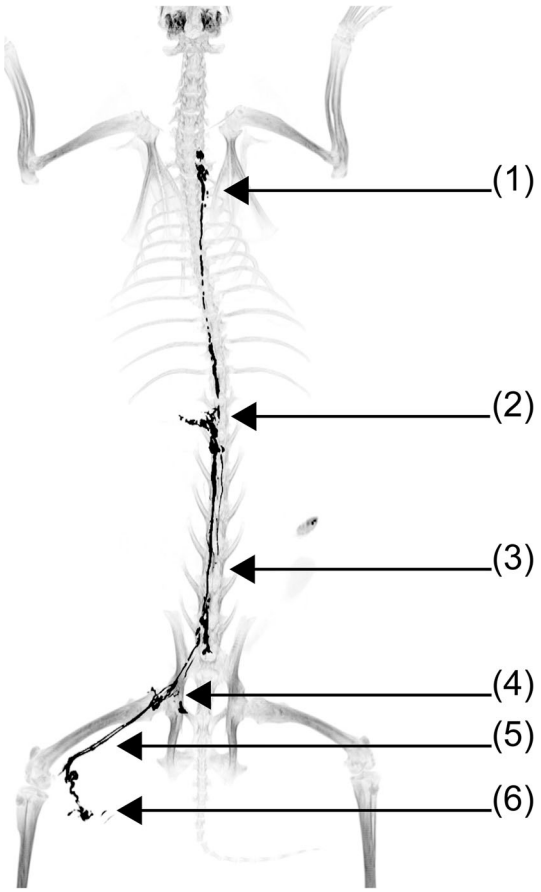

Fig. 5 Three-dimensional maximum intensity projection (3D MIP) image on post-lymphangiographic multidetector CT in anteroposterior view showing the lymphatic system in a rabbit: (1) thoracic duct, (2) cisterna chyli, (3) right lumbar lymphatic trunks, (4) right iliac lymphatic vessel, (5) right femoral lymphatic vessel, (6) right popliteal lymph node

Table 2 Degree of depiction of lymphatic system on 3D MIP

Rt. femoral lymphatic vessel	3.11 ± 1.32 (1–4)
Rt. iliac lymphatic vessel	2.78 ± 1.53 (1–4)
Rt. lumbar lymphatic trunks	2.33 ± 1.24 (1–4)
Lt. femoral lymphatic vessel	4 (4)
Lt. iliac lymphatic vessel	3.58 ± 0.51 (3–4)
Lt. lumbar lymphatic trunks	3.16 ± 1.03 (1–4)
Cisterna chyli	3.28 ± 0.83 (2–4)
Thoracic duct	2.33 ± 0.59 (1–3)

Data are presented as mean ± standard deviation (range)

Degree of depiction was graded by using a four-point visual score, in which a score of 1 indicated poor; a score of 2, faint; a score of 3, good; and a score of 4, excellent

3D MIP three-dimensional maximum intensity projection, *rt.* right, *lt.* left

Discussion

In our study, the popliteal lymph node could be rendered easily detectable by injecting 1% patent blue violet dyes into the bottom of the foot (90%). There was leakage of the total or a partial dose of Lipiodol around the popliteal lymph node in 78%. The main causes are as follows: The needle perforates the popliteal lymph node, Lipiodol may be forced back outside the needle because of its high viscosity, or the fast injection rate of Lipiodol may produce leakage. However, intranodal lymphangiography via the popliteal lymph node could be performed with a high success rate in the visualization of the lymphatics (89%). The advent of intranodal lymphangiography under ultrasound guidance [16–18] has clinically allowed lymphatic interventions to be much more easily performed and to be adopted more readily by interventional radiologists. Therefore, our outcome suggests that intranodal lymphangiography in rabbits would be able to be performed by interventional radiologists.

We chose lymphangiography using Lipiodol because intranodal lymphangiography using Lipiodol facilitates further preclinical lymphatic interventions in a rabbit model. Lipiodol, an oil-based contrast agent, remains for prolonged periods within the lymphatic structures, as opposed to water-based agents that easily leak out [19]. Generally, warming Lipiodol reduces its viscosity. Kora et al. [20] demonstrated that warming miriplatin–Lipiodol suspension to 40 °C reduces its viscosity to almost half of that at 25 °C. For this reason, Lipiodol was warmed to 40 °C in our study.

For thoracic duct embolization, which was first described by Cope and Kaiser where the thoracic duct is catheterized and subsequently embolized to treat chylothorax [8], the opacified cisterna chyli or retroperitoneal lymphatic duct is usually accessed through a transabdominal approach under fluoroscopic guidance [11]. In our study, visual scores of cisterna chyli were 3.28 ± 0.83. The Cohen kappa coefficient was 0.757–0.916. The distance between the body surface and cisterna chyli was 4.33 ± 0.14 cm. These results suggest that rabbits may be suitable for thoracic duct embolization following lymphangiography using Lipiodol.

In rabbits, the VX2 squamous tumor model, which is a longstanding model used in preclinical oncology studies, can be prepared. This animal tumor model may be used for imaging, as well as for the development of potential novel lymphatic interventions including intralymphatic agent delivery such as the use of chemotherapy, antibiotics and antigenic molecules, and potentiation of the immune system [21–23]. Itkin and Nadolski [23] predict that the potential for further growth of lymphatic interventions is vast and further development of lymphatic interventions will be a game-changing technique for patients suffering from numerous lymphatic diseases. Considering these aspects, lymphangiography and post-lymphangiographic MDCT in healthy rabbits in our study are useful for the development of further preclinical lymphatic interventions. However, to use a rabbit model for long-term study, further investigation regarding the tolerance volume of Lipiodol is required.

In conclusion, lymphangiography is feasible and the visibility of the lymphatic system on post-lymphangiographic MDCT in a rabbit model provides enough information for interventional radiologists to perform preclinical lymphatic interventions.

Acknowledgements We are grateful to Yoshiko Shinozaki and Sachie Tanaka of the Department of Laboratory Animal Science, the Education and Research Support Center, Tokai University for technical support, and staffs of the Department of Radiological Technology, Tokai University Hospital for taking MDCT images.

Funding This work was supported in part by JSPS KAKENHI (Grant No. JP16K19861) and 2015 Tokai University School of Medicine Research Aid.

Compliance with Ethical Standards

Conflict of interest The authors declare that they have no conflict of interest.

Ethical Approval All applicable international, national and institutional guidelines for the care and use of animals were followed. The study was approved by the institutional Animal Care and Use Committee of Tokai University.

References

1. Yamagami T, Masunami T, Kato T, Tanaka O, Hirota T, Nomoto T, et al. Spontaneous healing of chyle leakage after lymphangiography. Br J Radiol. 2005;78:854–7.
2. Kos S, Haueisen H, Lachmund U, Roeren T. Lymphangiography: forgotten tool or rising star in the diagnosis and therapy of postoperative lymphatic vessel leakage. Cardiovasc Intervent Radiol. 2007;30:968–73.
3. Matsumoto T, Yamagami T, Kato T, Hirota T, Yoshimatsu R, Masunami T, et al. The effectiveness of lymphangiography as a treatment method for various chyle leakages. Br J Radiol. 2009;82:286–90.
4. Alejandre-Lafont E, Krompiec C, Rau WS, Krombach GA. Effectiveness of therapeutic lymphography on lymphatic leakage. Acta Radiol. 2011;52:305–11.
5. Yoshimatsu R, Yamagami T, Miura H, Matsumoto T. Prediction of therapeutic effectiveness according to CT findings after therapeutic lymphangiography for lymphatic leakage. Jpn J Radiol. 2013;31:797–802.
6. Matsumoto T, Kudo T, Endo J, Hashida K, Tachibana N, Murakoshi T, et al. Transnodal lymphangiography and post-CT for protein-losing enteropathy in Noonan syndrome. Minim Invasive Ther Allied Technol. 2015;24:246–9.
7. Nadolski GJ, Chauhan NR, Itkin M. Lymphangiography and lymphatic embolization for the treatment of refractory chylous ascites. Cardiovasc Intervent Radiol. 2018;41:415–23.
8. Cope C, Kaiser LR. Management of unremitting chylothorax by percutaneous embolization and blockage of retroperitoneal lymphatic vessels in 42 patients. J Vasc Interv Radiol. 2002;13:1139–48.
9. Inoue M, Nakatsuka S, Yashiro H, Tamura M, Suyama Y, Tsukada J, et al. Lymphatic intervention for various types of lymphorrhea: access and treatment. Radiographics. 2016;36:2199–211.
10. Johnson OW, Chick JF, Chauhan NR, Fairchild AH, Fan CM, Stecker MS, et al. The thoracic duct: clinical importance, anatomic variation, imaging, and embolization. Eur Radiol. 2016;26:2482–93.
11. Toliyat M, Singh K, Sibley RC, Chamarthy M, Kalva SP, Pillai AK. Interventional radiology in the management of thoracic duct injuries: anatomy, techniques and results. Clin Imaging. 2017;42:183–92.
12. Pillay TG, Singh B. A review of traumatic chylothorax. Injury. 2016;47:545–50.
13. Kraitchman D, Kamel I, Weiss C, Georgiades C. Elucidation of percutaneously accessible lymph nodes in swine: a large animal model for interventional lymphatic research. J Vasc Interv Radiol. 2017;28:451–6.

14. Cope C. Percutaneous transabdominal embolization of thoracic duct lacerations in animals. J Vasc Interv Radiol. 1996;7:725–31.
15. Lymphography Tjernberg B. An animal study of the diagnosis of Vx2 carcinoma and inflammation. Acta Radiol Suppl. 1962;214:1–184.
16. Rajebi MR, Chaudry G, Padua HM, Dillon B, Yilmaz S, Arnold RW, et al. Intranodal lymphangiography: feasibility and preliminary experience in children. J Vasc Interv Radiol. 2011;22:1300–5.
17. Gomez FM, Martinez-Rodrigo J, Marti-Bonmati L, Santos E, Forner I, Lloret M, et al. Transnodal lymphangiography in the diagnosis and treatment of genital lymphedema. Cardiovasc Intervent Radiol. 2012;35:1488–91.
18. Nadolski GJ, Itkin M. Feasibility of ultrasound-guided intranodal lymphangiogram for thoracic duct embolization. J Vasc Interv Radiol. 2012;23:613–6.
19. Stecker MS, Fan CM. Lymphangiography for thoracic duct interventions. Tech Vasc Interv Radiol. 2016;19:277–85.
20. Kora S, Urakawa H, Mitsufuji T, Osame A, Higashihara H, Ohki T, et al. Warming effect on miriplatin-lipiodol suspension for potential use as a chemotherapeutic agent for transarterial chemoembolization of hepatocellular carcinoma: in vitro study. Hepatol Res. 2013;43:1100–4.
21. Yang Q, Wang XD, Chen J, Tian CX, Li HJ, Chen YJ, et al. A clinical study on regional lymphatic chemotherapy using an activated carbon nanoparticle-epirubicin in patients with breast cancer. Tumour Biol. 2012;33:2341–8.
22. Senti G, Kundig TM. Novel delivery routes for allergy immunotherapy: intralymphatic, epicutaneous, and intradermal. Immunol Allergy Clin North Am. 2016;36:25–37.
23. Itkin M, Nadolski GJ. Modern techniques of lymphangiography and interventions: current status and future development. Cardiovasc Intervent Radiol. 2018;41:366–76.